

The effect of masterbatch recipes on the homogenization properties of injection
molded parts

Zsíros L., Török D., Kovács J. G.

Accepted for publication in International Journal of Polymer Science

Published in 2017

DOI: [10.1155/2017/5745878](https://doi.org/10.1155/2017/5745878)

Research Article

The Effect of Masterbatch Recipes on the Homogenization Properties of Injection Molded Parts

László Zsíros, Dániel Török, and József Gábor Kovács

Department of Polymer Engineering, Faculty of Mechanical Engineering, Budapest University of Technology and Economics, Muegyetem Rkp. 3, Budapest 1111, Hungary

Correspondence should be addressed to József Gábor Kovács; kovacs@pt.bme.hu

Received 12 December 2016; Revised 8 March 2017; Accepted 29 March 2017; Published 3 May 2017

Academic Editor: Ulrich Maschke

Copyright © 2017 László Zsíros et al. This is an open access article distributed under the Creative Commons Attribution License, which permits unrestricted use, distribution, and reproduction in any medium, provided the original work is properly cited.

Appearance is a key factor in most injection molding applications. Unfortunately, there is no widespread method to objectively test visual appearance, such as color inhomogeneity of the parts or other surface defects. We developed an evaluation method to characterize the color inhomogeneity of injection molded parts. First, we examined manufacturing conditions and masterbatch recipes and then the individual effects of the components and their interactions on homogeneity.

1. Introduction

The majority of modern plastic products are made by injection molding. In most cases, the appearance of the product is extremely important and it can be greatly influenced by the coloring of the neat polymer. Since 90% of injection molding companies use solid-phase masterbatches to color their products [1], it is very important to investigate how they influence the appearance of the end product.

In addition to appearance, solid-phase masterbatches can also affect flame resistance, UV stability, and in certain cases mechanical properties. The color shade of a product is only one part of its appearance. Color evenness (whether there are any color inhomogeneity marks) is just as important. In the case of solid-phase masterbatches, the dispersion of the colorants can be critical [1, 2], but it is only one part of the total mixing process.

The homogenization of solid-phase masterbatches is influenced by several factors, such as the processing parameters [3], the design of the injection molding screw, the application of additional dynamic [4, 5] and static [6–8] mixers, and the properties of the material and masterbatch used to injection-mold the parts. The objective evaluation of the homogenization of various masterbatch recipes and components is an extremely important and a novel field of research.

Image processing is an important tool in homogeneity and color analysis. There are several methods to calculate

the homogeneity of images [9–11]. According to Cheng et al. [12], these methods can be categorized as follows: edge value-based methods [13], standard deviation (variance)-based calculations [14–16], and entropy-based calculations [17, 18]. Edge value-based methods usually apply a certain gradient operator on the pixels of the images, such as the Sobel operator, the Laplace operator, or the Robert operator. They use the gradient values above a given threshold. This way, the image can be segmented or certain formations can be detected. Entropy-based calculations evaluate image segmentation or contrast enhancements. Some calculation methods apply a combination of the above [10]. Even though a large number of different methods are used, mixing quality is usually evaluated by standard deviation or variance-based methods.

2. Methods

We investigated two different evaluation methods and compared the results with human visual inspections. 80 × 80 mm flat specimens were injection-molded and colored with nine different masterbatches. Each color was used with 7 different injection molding parameter combinations, which resulted in 63 different colors and homogeneity levels. In each of the 63 cases, 50 flat specimens were evaluated and their results were averaged. These results were compared to the average scores given by a group of 7 trained technicians inspecting the flat specimens with the same lighting.

First, the samples were evaluated with the variance-based measurement method developed by Zsíros et al. [19]. It consists of the following steps:

- (i) Injection molding of the test specimens
- (ii) Digitization of the samples
- (iii) Evaluation of the images with a special algorithm

The evaluation algorithm used the CIE Lab color coordinates ($P[L, a, b]$), since it is device-independent [20–22] and approximates human color difference sensation well [23]. The algorithm scans the image with a given window size and at every (i, j) position of this window the mean color coordinates are calculated ($\bar{a}_{i,j,k}$), where k is the size of the window. Window size (k) could be varied from 1 to the maximum size of the image. A matrix can be generated from the mean color coordinates as follows (see (1)):

$$\bar{\bar{A}}_{i,j,1} = \begin{bmatrix} \bar{a}_{0,0,1} & \bar{a}_{1,0,1} & \cdots & \bar{a}_{i-1,0,1} & \text{n.a.} \\ \bar{a}_{0,1,1} & \bar{a}_{1,1,1} & & \bar{a}_{i-1,1,1} & \text{n.a.} \\ \vdots & & \ddots & & \vdots \\ \bar{a}_{0,j-1,1} & \bar{a}_{1,j-1,1} & & \bar{a}_{i-1,j-1,1} & \text{n.a.} \\ \text{n.a.} & \text{n.a.} & \cdots & \text{n.a.} & \text{n.a.} \end{bmatrix}, \quad (1)$$

$$\bar{\bar{A}}_{i,j,k} = \begin{bmatrix} \bar{a}_{0,0,k} & \text{n.a.} & \cdots & \text{n.a.} \\ \text{n.a.} & \text{n.a.} & & \text{n.a.} \\ \vdots & & \ddots & \vdots \\ \text{n.a.} & \text{n.a.} & \cdots & \text{n.a.} \end{bmatrix},$$

where the elements of the matrix can be calculated as follows (see (2)):

$$\bar{a}_{i,j,k} = \frac{\sum_{x=i}^{i+k-1} \sum_{y=j}^{j+k-1} P[L, a, b](x, y)}{k^2}, \quad (2)$$

where i and j are the position of the moving window within the whole image, k is the width and height of the moving window, and x and y are the local coordinates within the moving window.

For all window sizes and positions, the Euclidean distances of each pixel from the mean color coordinates ($\bar{a}_{i,j,k}$) in the given window were calculated. For each window, the average Euclidean distance was calculated according to

$$\text{MD}_{i,j,k} = \frac{\sum_{x=i}^{i+k-1} \sum_{y=j}^{j+k-1} \sqrt{\sum_{\varepsilon=L,a,b} \{P[\varepsilon](x, y) - A[\varepsilon](x, y)\}^2}}{k^2}. \quad (3)$$

In the Lab color space, the distance of two colors is independent of the reference white; therefore, it was not necessary to measure that.

The lower the $\text{MD}_{i,j,k}$ value, the more even the color of the sample in the area covered by the moving window. Moving the window pixel by pixel, the software can locate the area

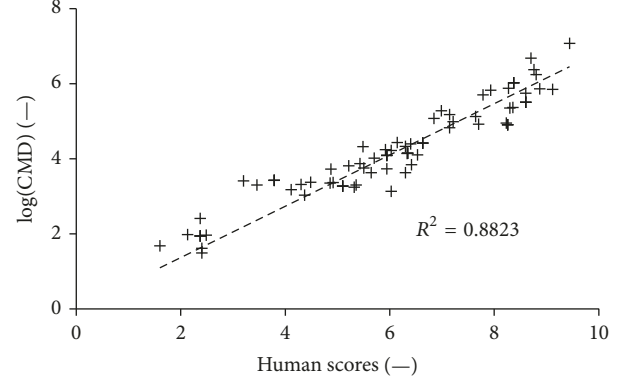


FIGURE 1: The correlation of the human scores and the software scores in the case of a 35-pixel window [24].

having the highest MD_k value (HMD_k). If the size of the moving window is equal to the image size in pixels, a global MD value (GMD) can be obtained. The software calculates the HMD_k values for different window sizes and corrects this value with the noise of the image (GMD). These corrected values (CMD) are calculated from HMD and GMD values according to

$$\text{CMD} = \text{HMD} - \text{GMD}. \quad (4)$$

Zsíros et al. found that, at a certain window size, the logarithm of the CMD values is proportional to human visual homogeneity perception. Therefore, the main advantage of this evaluation method is that it produces inhomogeneity scores that correlate very well with conventional, visual evaluation methods (Figure 1) [24]. This can also be interpreted as the proof of the Weber-Fechner law [25] and its application to human inhomogeneity sensation.

The inhomogeneity of the samples was also calculated with an algorithm based on the edge value method. The steps of the measuring process are the same as those of the variance-based method mentioned before. The digitized images, however, have considerable noise to which this kind of evaluation is sensitive. Therefore, the noise of the images has to be reduced before evaluation, for which an image-blurring filter [26] was used. The type of filter was weighted spatial averaging filter (see (5)):

$$\bar{\bar{F}}(x, y) = \begin{bmatrix} 0,071 & 0,1 & 0,071 \\ 0,1 & 0,316 & 0,1 \\ 0,071 & 0,1 & 0,071 \end{bmatrix}. \quad (5)$$

The color values of the filtered image are produced by the 2D discrete convolution of the matrix of the color values of the original image and the spatial averaging mask (see (6)):

$$\bar{\bar{A}}[L, a, b](x, y) = \bar{I}[L, a, b](x, y) \otimes \bar{\bar{F}}(x, y), \quad (6)$$

where $A[L, a, b](x, y)$ is the matrix of the color values of the filtered image, while $I[L, a, b](x, y)$ is the matrix containing the color values of the original image, and $F(x, y)$ is the

matrix used for the filtering of the image. Next, the color change is calculated in every pixel of the image, in every color

channel. The gradient matrices of the image are calculated from the color values according to

$$\begin{aligned} \overline{B}[L, a, b](i, j) &= \sum_{i=2}^{n-1} \sum_{j=2}^{m-1} \sqrt{\left[\frac{(A[L, a, b](i-1, j) - A[L, a, b](i+1, j))}{2} \right]^2 + \left[\frac{(A[L, a, b](i, j-1) - A[L, a, b](i, j+1))}{2} \right]^2}, \quad (7) \end{aligned}$$

where $B[L, a, b](i, j)$ is the gradient matrix, $A[L, a, b](i, j)$ is the color value (L, a, b) matrix of the digitized image, and n and m are the width and the height of the image in pixels.

Inhomogeneity is defined as the summation of the elements of the $B[L, a, b]$ matrix divided by the area of the picture. The error value is multiplied by 100 to make the two scales approximately the same; therefore, they can be better compared. The images are characterized by the values of the L color channel as inhomogeneity is higher in this color channel than in the others.

The calculation results based on standard deviation (Figure 1) and edge value (Figure 2) show different correlations with human inspection. The square of the correlation based on standard deviation is 0.882, while in the case of the edge value-based method it is 0.735. Since our goal was to use a method which has high correlation with human inspection, we used the standard deviation-based method used by Zsíros et al. [19].

3. Materials

Masterbatches usually consist of at least 5–8 components, such as the carrier, the coloring agents, and special additives. The carrier has to be chemically compatible with the polymer that needs to be colored. Color matching usually requires 3–4 coloring agents. These coloring agents can be dyes or organic or inorganic pigments. In addition, special additives are added to some of the masterbatches to improve processability or serve as a wetting agent or dispersing aid or provide special properties, such as higher crystallinity or inflammability. The same color can be achieved with different coloring agents, which can result in significant differences in the homogenization properties. Figure 3 shows the homogeneity of different injection molded pink test specimens. The color difference between these test specimens can be neglected ($\Delta E < 1$). Although the color shades of the specimens were similar, their homogeneities showed a significant difference. This difference can be attributed to numerous factors, such as the recipe of the masterbatch, its manufacturing conditions, the properties of the components of the masterbatch, and the interaction between the components. To see the effects of the different masterbatch processing conditions, we compared two masterbatches. One of them was compounded on a special twin-screw extruder designed for masterbatch production, and the other was compounded on a LabTech corotating twin-screw extruder ($L/D = 44$, screw diameter: $\varnothing 26$ mm, max. temp.: 400°C , max. screw rotation speed: 800 rpm).

The masterbatches which had the same composition but were processed on different twin-screw extruders and under different conditions did not show significant differences in their homogenization properties (Figure 3).

After these tests, two additional test series were executed and evaluated. In the first test series, we tested six different masterbatches that only contained one type of pigment (organic or inorganic) or dye besides the carrier. The masterbatches tested in these test series were prepared in the factory of a multinational masterbatch manufacturing company with the same processing conditions. Injection molded flat specimens were produced with identical processing parameters from ABS, Styrolution GP 35 as raw material, and the carrier of the masterbatch was also ABS, Styrolution GP 35 in all cases. The tested pigments and dyes were color components of the original pink color. The injection molded plates were scanned and evaluated with the variance-based algorithm described in the Methods. All types of colorants (dyes, organic and inorganic pigments) are usually applied in a typical concentration range. In this test series, the concentrations of the components were the approximate averages of these ranges, as shown in Table 1, where *Red Dye* means that this specific monobatch contained only a red dye as a colorant besides the carrier. *Red O* stands for a monobatch containing red organic pigments, while *Red IO* stands for a monobatch containing red inorganic pigments only. The same applies to *Blue Dye*, *Blue O*, and *Blue IO* monobatches.

The commercial names and the suppliers of the different pigments and dyes can be seen in Table 2.

In the second test series, we tested eight different recipes including the original masterbatch, to compare the effects of two different TiO_2 types (rutile and anatase), three different additives, a higher concentration of one additive, the different colorant types (dye and organic pigments), and the effect of a wetting agent in the case of organic pigments. The compositions of the masterbatches tested in the second test series are shown in Table 3.

The original masterbatch recipe was modified in several steps, and in each case only one component was changed. Either the content of a component was modified or it was replaced with a different one. From these masterbatches, flat specimens were injection-molded similar to those in the first test series, followed by digitization and homogeneity measurements. Finally, their results were compared to the homogeneity of the test specimens made with the original masterbatch.

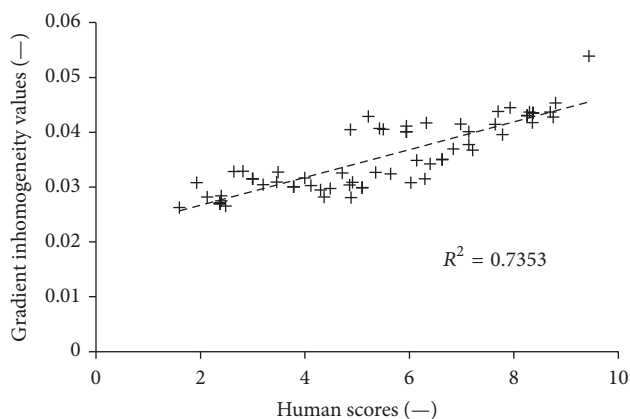


FIGURE 2: The correlation of the human scores and the edge value-based method.

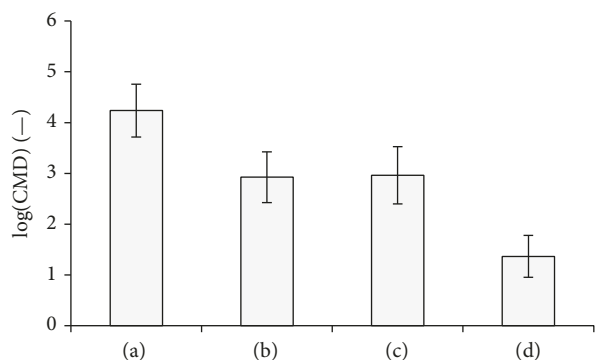


FIGURE 3: The homogeneity differences between injection molded test specimens: (a) original masterbatch, (b) modified masterbatch produced on a special extruder, (c) modified masterbatch produced on the LabTech corotating twin-screw extruder, and (d) compounded material.

TABLE 1: The different colorants and their concentrations in the masterbatches of the first test series.

	1	2	3	4	5	6
Red Dye	1.00%					
Red O		5.00%				
Red IO			10.00%			
Blue Dye				1.00%		
Blue O					5.00%	
Blue IO						10.00%

4. Results and Discussion

The measurement results of the first test series are in Figure 4. The individual inhomogeneity levels of the various colorants showed some significant differences, but this does not explain the variation of the homogenization properties of the different masterbatch recipes. The standard deviations showed bigger differences, which means that in the case of series 1/sample 3 and series 1/sample 4 there is a little difference between samples in the same series, while in the case of series

TABLE 2: The types and suppliers of the tested coloring agents.

	Raw material	Supplier
Red Dye	Macrolex Red EG	Lanxess
Red O	Cinilex DPP SR2P	Cinic
Red IO	Bayferrox 130	Bayer
Blue Dye	Keyplast Blue KR	Keystone
Blue O	Heliogen K6902	BASF
Blue IO	Ultramarine NI-12	Nubiola

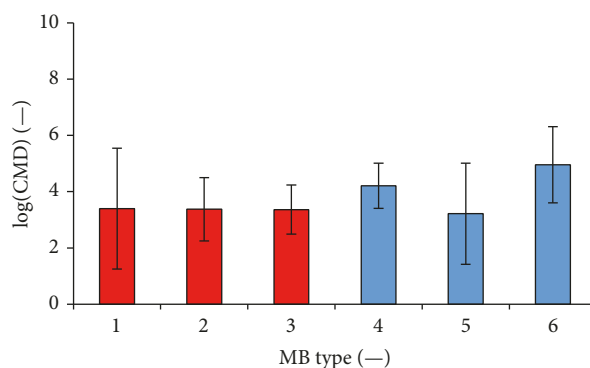


FIGURE 4: Inhomogeneity scores of the tested masterbatches in the first test series (1: Red Dye; 2: Red Organic; 3: Red Inorganic; 4: Blue Dye; 5: Blue Organic; 6: Blue Inorganic).

1/sample 1 and series 1/sample 5 there was a larger difference within the series than between the averages of the two series.

Masterbatch series 1/sample 3 and series 1/sample 4 are better due to their lower standard deviations; in other words, there is a smaller difference between the samples within the series. However, the variations in the homogenization properties of the different masterbatches cannot be explained with these differences in Figure 4. This means that the inhomogeneities in the various masterbatches are not caused by the individual components but by the interactions between them. In this case, the color evenness of a masterbatch formulated from the colorant of series 1/sample 3 and series 1/sample 4 cannot be calculated with the rule of mixtures as the interaction of the two materials is unknown.

In the second test series, first three different additives were tested (Figure 5). These additives were potential dispersing aids, which should have influenced the masterbatch homogenization properties. They were added to the masterbatch in the same m/m% ratio. They contained the same colorant types as the original masterbatch (rutile type TiO_2 and a dye) besides the different additives. They did not influence the homogeneity of the injection molded parts; thus, the type of the additive to be used should be determined with another method.

After testing the different additive types (A1, A2, and A3), we added additive A1 to the masterbatch in a significantly higher concentration. The usual concentration of this additive is 0.5 m/m% but in this case it was 8 m/m%. The differences in the homogeneity scores were tested with a two-sample *t*-test. It did not show significant differences between the two masterbatches.

TABLE 3: The compositions of the masterbatches in the second test series.

	1	2	3	4	5	6	7	8
Colorant type	Dye	Dye	Dye	Dye	Dye	Organic	Organic	Organic
TiO ₂ type	Rutile	Rutile	Rutile	Rutile	Anatase	Rutile	Rutile	Rutile
Wetting agent	0%	0%	0%	0%	0%	0%	10%	2,5%
Additive type	A1	A2	A3	A1	A1	—	—	—
Additive cont.	0.5%	0.5%	0.5%	8%	0.5%	0%	0%	0%

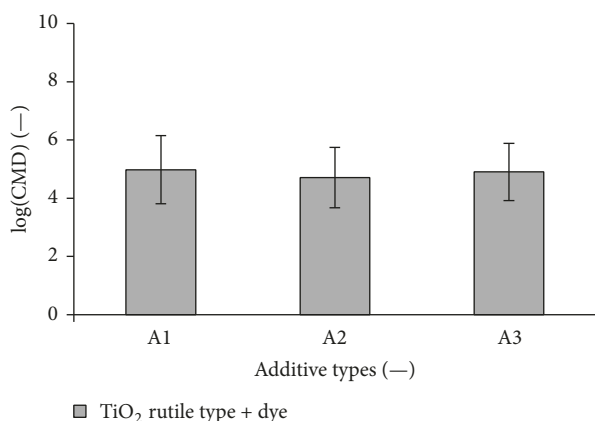


FIGURE 5: The effect of the different additives.

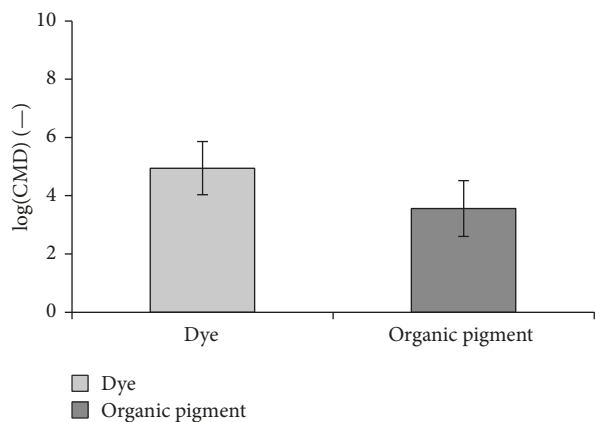


FIGURE 6: The effect of colorant type.

Next, the original dye-based pink masterbatch was modified and tested with two different types (rutile and anatase) of TiO₂. Results were tested with two-sample *t*-tests again, which showed no significant homogeneity differences between the two masterbatches.

After this, the effect of colorant type was investigated. The original pink masterbatch was recreated with different dyes. This was compared to a masterbatch containing organic pigments instead of dyes. The organic pigments significantly reduced color inhomogeneities in the samples, as shown in Figure 6. Although organic pigments and dyes have very similar homogenization properties in monobatches, they behaved differently due to their interaction with the other components.

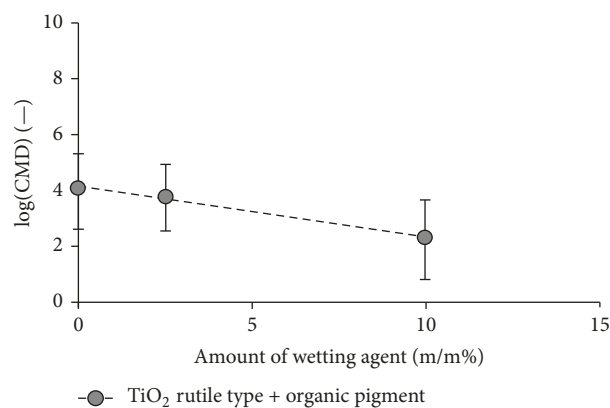


FIGURE 7: The effect of the amount of wetting agent.

Next, 2.5 m/m% and 10 m/m% wetting agents were added to the organic pigment-based pink masterbatch (Figure 7). The homogenization properties further improved, and in the case of the masterbatch containing 10 m/m% wetting agent the inhomogeneity scores were the lowest of all masterbatches tested. The significance of the difference between the masterbatch containing 10 m/m% wetting agent and the masterbatch containing 0 m/m% wetting agent was verified with a two-sample *t*-test and it was significant. Although the effects of the wetting agent were only tested with rutile type TiO₂ (Figure 7), we expect that the effects with the anatase type would be similar, since measurements did not show any differences in the behavior of rutile and anatase type TiO₂ in the investigated masterbatch compositions.

The influence of the wetting agent on homogenization properties could be further investigated with different wetting agent concentrations to see whether it is a linear decline (as shown in Figure 7) or follows a saturation pattern. It would also be interesting to see how the different types of TiO₂ behave in an organic pigment-based masterbatch. The results with the dye-based masterbatches suggest that they will not have a significant influence, but due to the possible cross-effects, it requires further investigation. Wetting agents are typically applied in the case of organic pigment-based masterbatches, but their effect could be tested in the case of the original dye-based masterbatches as well.

5. Conclusions

To evaluate the homogeneity of injection molded flat specimens, a variance-based homogeneity calculation method was applied, and it was shown that this model correlates well with

human visual inspections ($R^2 = 0.882$). In our preliminary tests, we proved that it is the recipe of the masterbatch and not its manufacturing technology that causes the differences in the homogeneity of the molded samples. Based on this, we conducted two test series. In the first test series, six monobatches were investigated. Each of them contained only one type of pigment or dye besides the carrier. The color homogeneity scores of the injection molded flat specimens colored with these masterbatches did show some minor differences, but these cannot explain the larger differences obtained in the different masterbatch recipes. Therefore, the inhomogeneities of the injection molded parts colored with solid-phase masterbatches are caused not only by the individual components of the masterbatches but also by the interactions between them. In the second test series, the interactions of the components were investigated, and in each test only one component or its concentration was modified and then compared to the original recipe. In our TiO₂-based masterbatches, color homogeneity became better if organic pigments were used instead of dyes, and it could be further improved if a wetting agent (up to 10 m/m%) was added to that masterbatch. Furthermore, we tested the effects of two different types of TiO₂, three different additives, and the increased amount of additive on homogenization properties. These modifications did not show any significant effect on the homogeneity of the injection molded flat specimens.

Conflicts of Interest

The authors declare no conflicts of interest regarding the publication of this paper.

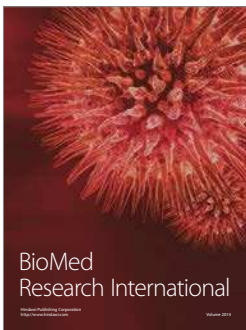
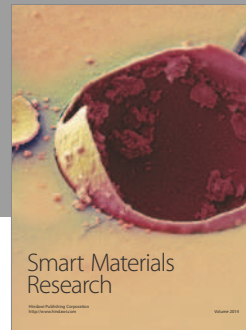
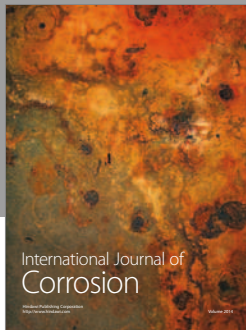
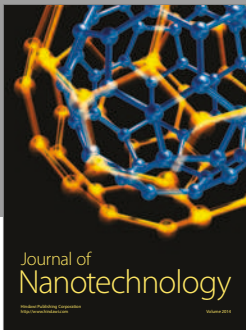
Acknowledgments

The authors wish to thank Arburg Hungária Kft. for the Arburg Allrounder 370S 700-290 injection molding machine, Lenkes GmbH for the clamping tool system, and Piován Hungary Kft. for their support.

References

- [1] A. Müller, *Coloring of Plastics*, Carl Hanser Verlag, Munich, Germany, 2003.
- [2] C. Rauwendaal, *Polymer Mixing: Self-Study Guide*, Carl Hanser Verlag, Munich, Germany, 1998.
- [3] L. Zsíros and J. G. Kovács, "Measuring color inhomogeneity of injection molded parts," in *Proceedings of OGÉT*, Arad, Romania, 2013.
- [4] L. Zsíros and J. G. Kovács, "Optimization of homogenizing capacity of injection moulding machines," *Rubber and Plastic*, vol. 50, no. 9, pp. 347–350, 2013.
- [5] R. S. Hindmarch, "The cavity transfer mixer: a blender for all seasonings," *Materials and Design*, vol. 8, no. 6, pp. 331–339, 1987.
- [6] D. Török, L. Zsíros, and J. G. Kovács, "Investigation of StaMixCo static mixers with different number of mixing elements and diameter," *Rubber and Plastic*, vol. 51, no. 9, pp. 346–351, 2014.
- [7] R. K. Thakur, C. h. Vial, K. D. P. Nigam, E. B. Nauman, and G. Djelveh, "Static mixers in the process industries—a review," *Trans IChemE Part A*, vol. 81, pp. 787–826, 2003.
- [8] H. E. H. Meijer, M. K. Singh, and P. D. Anderson, "On the performance of static mixers: a quantitative comparison," *Progress in Polymer Science*, vol. 37, no. 10, pp. 1333–1349, 2012.
- [9] S. Karami, M. Imani, and F. Farahmandghavi, "A novel image analysis approach for evaluation of mixing uniformity in drug-filled silicone rubber matrix," *International Journal of Pharmaceutics*, vol. 460, no. 1-2, pp. 158–164, 2014.
- [10] X.-Y. Wang, T. Wang, and J. Bu, "Color image segmentation using pixel wise support vector machine classification," *Pattern Recognition*, vol. 44, no. 4, pp. 777–787, 2011.
- [11] J. G. Rosas and M. Blanco, "A criterion for assessing homogeneity distribution in hyperspectral images. Part 1: homogeneity index bases and blending processes," *Journal of Pharmaceutical and Biomedical Analysis*, vol. 70, pp. 680–690, 2012.
- [12] H. D. Cheng, M. Xue, and X. J. Shi, "Contrast enhancement based on a novel homogeneity measurement," *Pattern Recognition*, vol. 36, no. 11, pp. 2687–2697, 2003.
- [13] R. C. Hardie and C. G. Boncelet, "Gradient-based edge detection using nonlinear edge enhancing prefilters," *IEEE Transactions on Image Processing*, vol. 4, no. 11, pp. 1572–1577, 1995.
- [14] B. Daumann and H. Nirschl, "Assessment of the mixing efficiency of solid mixtures by means of image analysis," *Powder Technology*, vol. 182, no. 3, pp. 415–423, 2008.
- [15] X. Liu, C. Zhang, and J. Zhan, "Quantitative comparison of image analysis methods for particle mixing in rotary drums," *Powder Technology*, vol. 282, pp. 32–36, 2015.
- [16] P. Shenoy, F. Innings, T. Lilliebjelke, C. Jonsson, J. Fitzpatrick, and L. Ahrné, "Investigation of the application of digital colour imaging to assess the mixture quality of binary food powder mixes," *Journal of Food Engineering*, vol. 128, pp. 140–145, 2014.
- [17] W. K. Lai, I. M. Khan, and G. S. Poh, "Weighted entropy-based measure for image segmentation," vol. 41, pp. 1261–1267.
- [18] J. F. Khan and S. M. Bhuiyan, "Weighted entropy for segmentation evaluation," *Optics and Laser Technology*, vol. 57, pp. 236–242, 2014.
- [19] L. Zsíros, A. Suplicz, G. Romhány, T. Tábi, and J. G. Kovács, "Development of a novel color inhomogeneity test method for injection molded parts," *Polymer Testing*, vol. 37, pp. 112–116, 2014.
- [20] K. L. Yam and S. E. Papadakis, "A simple digital imaging method for measuring and analyzing color of food surfaces," *Journal of Food Engineering*, vol. 61, no. 1, pp. 137–142, 2004.
- [21] R. E. Larraín, D. M. Schaefer, and J. D. Reed, "Use of digital images to estimate CIE color coordinates of beef," *Food Research International*, vol. 41, no. 4, pp. 380–385, 2008.
- [22] F. Mendoza, P. Dejmeq, and J. M. Aguilera, "Calibrated color measurements of agricultural foods using image analysis," *Post-harvest Biol. Technol.*, vol. 41, no. 3, pp. 285–295, 2006.
- [23] R. Abrams, M. Ali, P. Denton, J. A. Igualada, M. Groen, and E. Gschwind, "Coloring plastics: fundamentals and trends," *Plastics, Additives and Compounding*, vol. 3, pp. 18–25, 2001.
- [24] L. Zsíros, D. Török, and J. G. Kovács, "Development of a color inhomogeneity measurement method and its application to the evaluation of static mixers," in *Proceedings of OGÉT*, Csíksomlyó, Romania, 2015.

- [25] S. Dehaene, "The neural basis of the weber-fechner law: a logarithmic mental number line," *Trends in Cognitive Sciences*, vol. 7, no. 4, pp. 145–147, 2003.
- [26] S. G. Hoggar, *Mathematics of digital images*, Cambridge University Press, New York, NY, USA, 2006.



Hindawi

Submit your manuscripts at
<https://www.hindawi.com>

